Transactions of the Materials Research Society of Japan 25 [2] 601-604 (2000)

Ionic Conductivity at Interfaces in Yttria-Stabilized Zirconia: A Computer Simulation Study

C. A. J. FISHER and H. MATSUBARA
Japan Fine Ceramics Center, 2-4-1 Mutsuno, Atsuta-ku, Nagoya
Fax: +81-52-871-3599, e-mail: fisher@jfcc.or.jp

We have examined three grain boundaries and three surfaces of cubic 8 mol% yttria-stabilized zirconia via molecular dynamics simulations in an attempt to better understand the influence of microstructure on anionic conductivity in this material. The atomic interactions were described by a two-body Born-Mayer function in systems of 1000 to 2500 atoms. The simulated temperature in the case of grain boundaries was 1273 K, and for surfaces, 1773 K. The three grain boundaries investigated were the Σ5 and Σ13 symmetrical tilt boundaries and the Σ3 (111) θ=60° symmetrical twist boundary. The two tilt boundaries both increased the resistance of the system relative to a single crystal, but the twist boundary showed slightly higher conductivity due to the high degree of disorder of anions in the boundary region. Three surfaces were constructed by slicing single crystals parallel to the (111), (110) and (112) planes. The (111) surface supported an oxygen diffusion rate greater than in the bulk, while the (110) and (112) surfaces decreased the overall ionic conductivity.
Key words: YSZ, oxide ion conductivity, molecular dynamics, interface

1. INTRODUCTION

Impedance spectroscopy studies have shown that interfaces in polycrystalline cubic zirconia are more resistive to oxide ion conduction than the crystalline grain interiors, even in nominally pure materials[1-4]. Minimizing this resistance is one possibility of improving the performance of zirconia, which is used as a solid electrolyte in oxygen gas sensors, ceramic fuel cells and other devices[5]. Unlike impedance spectroscopy, which only reveals the effect of the overall or average interface structure, simulation techniques such as the molecular dynamics (MD) method allow us to probe systems on the atomic level. Hence we have performed MD calculations of various surfaces and grain boundaries in yttria-stabilized zirconia (YSZ) to better understand the role of microstructure on oxide ion conductivity in this material.

A number of atomistic simulations of grain boundaries[6] and surfaces[6-10] of cubic zirconia have been reported in the literature. These were all performed at zero Kelvin using either the static lattice / energy minimization technique, or, in one case (ref. 10), density functional theory. In this paper we extend our work on grain boundary structures in zirconia[11-13] to include the first study of oxide ion transport in crystal surface regions of this material by the MD method.

2. SIMULATION METHOD

The interactions between ions were based on the Born model of polar solids in which forces are two-body and dependent only on the distances between particles. The effective potential function, $\phi(r)$, was a combination of the Coulomb energy and a short-range component of the Buckingham form:

$$\phi(r_{ij}) = \frac{q_i q_j}{r_{ij}} + A\exp(-\frac{\rho}{r_{ij}}) - \frac{C}{r_{ij}^6} \qquad (1)$$

where A, ρ and C are parameters particular to interactions between two ions i and j of charges q_i and q_j, respectively, separated by distance r_{ij}. The exponential term approximates the effect of electronic repulsion at small separations, and the inverse term any dispersion forces that may be present. In this study, we used the potential parameters of Lewis and Catlow[14], as these successfully reproduce the lattice parameters and cell geometry of cubic YSZ to within a few percent. All simulations were performed using the MOLDY code[15].

Grain boundaries and surfaces of 8 mol% YSZ (8YSZ) were simulated at temperatures of 1273 and 1773 K, respectively. The initial grain boundary configurations were constructed according to CSL theory[16] by taking two ZrO_2 single crystals and tilting or twisting one of them by a given angle, θ, relative to the other until a fraction ($1/\Sigma$) of the atomic sites of both crystals coincided. Three symmetrical boundaries were simulated - Σ5 (310) / [001] and Σ13 (320) / [001] tilt boundaries, and a Σ3 (111) twist boundary, with misorientation angles, θ, of 36.9°, 22.6° and 60°, respectively. A number of Y^{3+} ions were then randomly substituted for Zr^{4+} ions to form systems of 8YSZ, and the corresponding number of O^{2-} ions removed to maintain zero net charge. Grain boundary systems contained between 1873 and 2387 ions, while the surface simulations contained between 1141 and 1741 ions.

Surfaces were formed by truncating single crystals of 8YSZ along a specified plane - (111), (110) or (112) - at two positions to form a slab geometry. In both grain boundary and surface simulations, the box dimensions in the plane of the interface were held constant based on the equilibrium crystal lattice parameters to take into account the constraining effect of the bulk crystal on the interface.

Each configuration was placed in a simulation box extended in the z direction (perpendicular to the interface) so that mirror images of the interfaces did not interact with each other after applying 3D periodic boundary conditions. During equilibration of grain boundary systems, the simulation box was permitted to expand or contract in the z direction to accommodate changes in grain boundary volume.

Particle positions were periodically recorded during simulation runs of 60 000 time steps of 2 fs each to allow calculation of transport properties, in particular the mean square displacement (*msd*), after the simulation run had finished. The *msd* of a species numbering N particles is defined as:

$$msd = \frac{1}{N}\sum_{n=1}^{N}\langle(\mathbf{r}_n(t_o+t)-\mathbf{r}_n(t_o))^2\rangle \qquad (2)$$

where the angular brackets are taken to indicate an ensemble average over all possible initial times, t_0, and $r_i(t)$ is the position of ion i at time t. The *msd* gives a measure of the diffusion undergone by a particular species during the course of the simulation. According to the Einstein equation, the gradient of a plot of *msd* versus time is proportional to the diffusion coefficient, which is itself proportional to the ionic conductivity, σ, according to the Nernst-Einstein relation.

3. RESULTS AND DISCUSSION

3.1 Grain Boundaries

The structures of the Σ5 tilt, Σ13 tilt, and Σ3 twist grain boundaries[13] in cubic ZrO_2 were calculated by averaging atom positions over the course of simulation runs, and are shown in Fig. 1. The structure of the Σ5 symmetrical tilt boundary is in excellent agreement with an HRTEM micrograph published recently[17], with a grain boundary width of ≈ 1 nm. This demonstrates the usefulness of our method for predicting microstructures, and gives us confidence that our simulation results are indeed reliable.

In Table I we report energy terms calculated for the three grain boundaries of 8YSZ considered here. While these values are associated with large uncertainties, they do reveal trends in the grain boundaries' properties. Comparing the excess volumes in Table I shows us that the twist boundary has a much higher density of atoms than the tilt boundaries. Furthermore, while the twist boundary is the most stable, it is also the easiest to fracture owing to its low binding energy. This is reasonable considering that it is formed from two (111) planes, which is the most stable surface of cubic YSZ, as discussed in the next section.

Table I: Calculated properties of grain boundaries.

Boundary	Excess Volume (%)	Formation Energy (J/m^2)	Binding Energy (J/m^2)
Σ5 tilt	1.1	2.2	4.3
Σ13 tilt	0.8	1.7	-
Σ3 twist	0.3	1.2	1.2

The oxygen diffusion behavior of each of the boundaries is summarized as plots of overall system *msd* versus time (Fig. 2). The *msd* of a single crystal (S.C.) of 8YSZ is included for comparison. This figure reveals that, while the two tilt boundaries support lower diffusion rates than the single crystal, and hence degrade the overall conductivity, the twist boundary displays slightly higher conductivity. This is due to the special geometry of the Σ3 (111) 60° twist boundary, in which the two cation sublattices fortuitously coincide, thereby forming a stable, undisrupted sublattice. In contrast, the oxygen ions at the boundary are in a disordered and highly mobile state due to their close proximity. It is not yet clear whether rapid oxygen diffusion will be displayed by other, more general, twist boundaries.

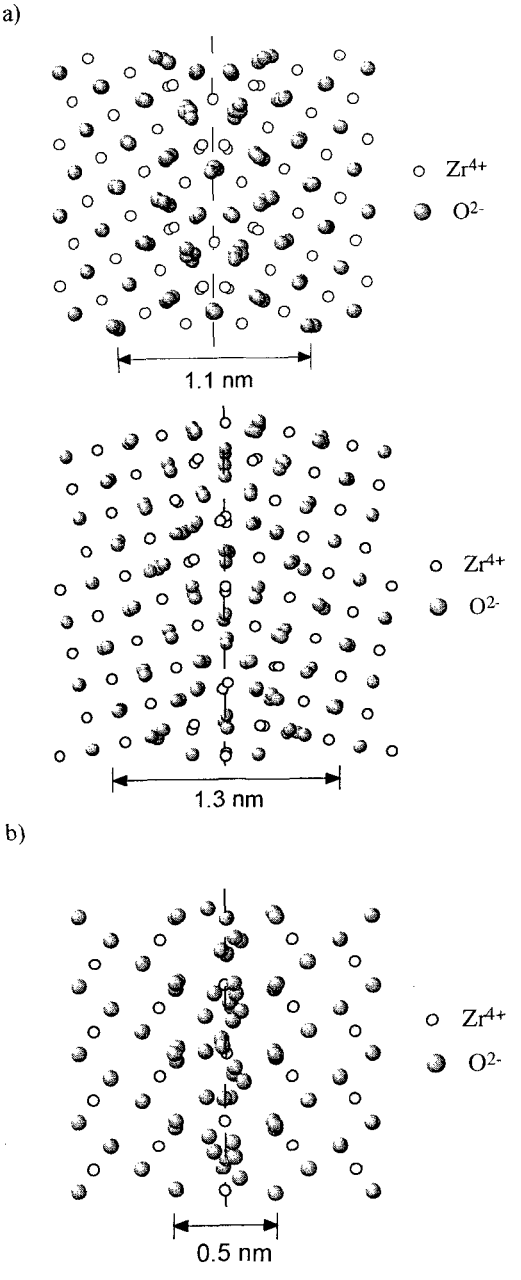

Fig. 1: Structures of a) Σ5 tilt, b) Σ13 tilt, and c) Σ3 twist grain boundaries.

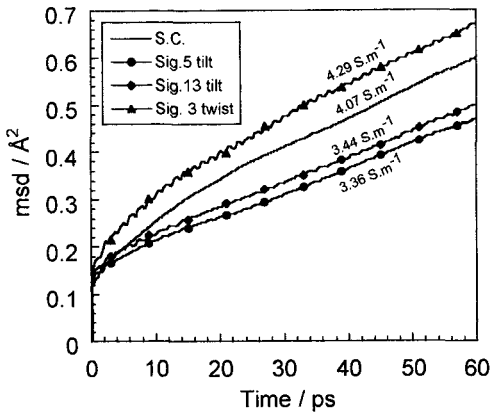

Fig. 2: Mean square displacements (*msd*s) and conductivities for the various grain boundary systems.

3.2 Surfaces

The {110} and {112} surfaces of the cubic fluorite structure are Type I faces[18], with stoichiometric numbers of cations and anions in each plane, whereas the {111} surface is a Type II face[18]. The relaxed structure, however, can change significantly from the "ideal" truncated structure, strongly affecting surface properties such as energy states and atomic diffusion.

The two Type I surfaces were found to exhibit surface rumpling, with oxygen ions extending out of the surface plane. A similar observation was made by Mackrodt when simulating the (110) surface of ZrO_2[7]. The (112) surface showed even greater rumpling than the (110), however, with half the anions at the surface moving above and covering what were the exposed cations on the unrelaxed surface. In contrast, the Type II surface showed little or no rumpling.

These changes in surface structure upon relaxation are reflected in the calculated surface energies, shown in Table II. The most stable surface was found to be the (111) surface, in agreement with previous simulation results[7-9], and also the observed morphology of cubic zirconia crystals. However, our surface energy values are about twice as large as those measured for cubic calcia stabilized zirconia[19] at 1773 K by the multiphase equilibration technique, which we attribute to neglect of entropy terms in our calculation.

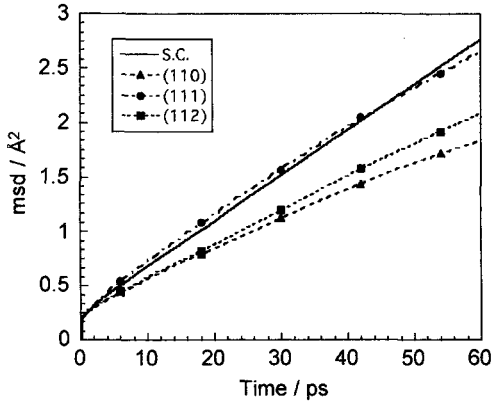

Fig. 3: Total O^{2-} *msd*s of surface systems compared with a single crystal (S.C.) of 8YSZ at 1773 K.

Fig. 3 shows the overall *msd*s of anions calculated from the three surface-containing systems of 8YSZ at 1773 K compared with an infinite (edgeless) single crystal (S.C.). The *msd*s of Y^{3+} and Zr^{4+} cations are not included because they simply reveal that ions at the surface have greater vibrational amplitudes than bulk ions, with no diffusion taking place. The anions, however, do diffuse, as shown by the increasing *msd*s in Fig. 3. Whereas the (111) surface supports essentially the same rate of diffusion as the single crystal, the two Type I surfaces have lower diffusion rates, and hence lower oxygen conductivities.

Table II: Calculated surface energies at 1773 K.

Surface	Surface Energy (J/m^2)
(111)	1.2
(110)	2.2
(112)	2.1

Since the overall *msd*s are weighted in favor of the system containing the higher volume of bulk crystal, we also calculated *msd*s layer by layer for crystal planes parallel to the surfaces. In Fig. 4 we plot the oxygen *msd*s calculated for bulk (b) and surface (s) regions of each system. Since oxygen diffusion at the outermost layer is restricted in the direction pointing into the vacuum, only one of the *msd* components parallel to the surface plane is shown.

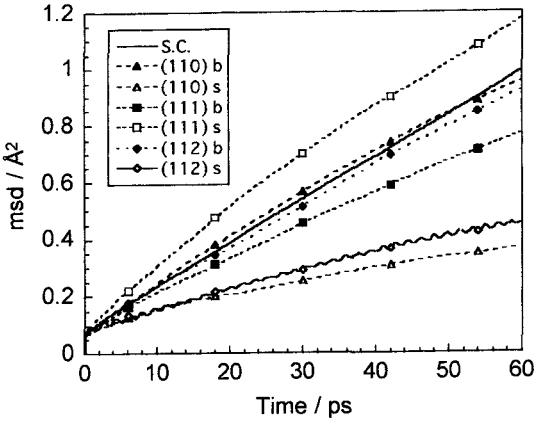

Fig. 4: Components of O^{2-} *msd*s parallel to surface plane for bulk (b) and surface (s) regions.

For the Type I faces, although the bulk crystal conducts anions as rapidly as an infinite single crystal, the surface regions show much lower diffusion rates. The (111) surface, in contrast, shows *faster* diffusion at the surface than in the bulk. The reason for the lower diffusion rate in the bulk region of the (111) system compared to an infinite single crystal is that it actually contains a couple of crystal layers immediately below the outermost surface layers which have conductivities *lower* than the "true" inner crystalline bulk. The net result is that the total *msd* (surface + bulk) of the (111) system approaches that of an edgeless single crystal, as shown in Fig. 3.

The results of Fig. 4 are strong evidence that the variation in structure of the surfaces results in conductivity gradients between the bulk and surface layers. Further simulations are underway to understand the reasons for these changes in conductivity more precisely, but it is expected to be a function of the relative dilation/contraction of crystal planes relative to the bulk crystal.

4. CONCLUSIONS

Our MD simulations have demonstrated that the specific oxide ion conductivity in YSZ depends on he interface structure and orientation. More precisely, the following conclusions can be drawn:

a) the good correspondence between the predicted and experimentally observed structure of the Σ5 tilt grain boundary gives us confidence that our potentials and method for modeling interfaces are reliable.

b) the two representative symmetrical tilt boundaries studied here - Σ5 and Σ13 - have lower oxygen diffusion rates than the bulk crystal, and thus decrease the overall conductivity of 8 YSZ.

c) the Σ3 twist boundary displays higher diffusion rates than the bulk, and thus improves the overall oxide ion conductivity,

d) the (110) and (112) surfaces decrease the overall conductivity of cubic YSZ grains.

e) the (111) surface shows slightly higher oxygen conductivity than the bulk crystal due to lattice expansion in the surface layers.

5. REFERENCES

[1] M. J. Verkerk, B. J. Middelhuis and A. J. Burggraaf, *Solid State Ionics*, **6**, 159-70 (1982).

[2] B. C. H. Steele and E. P. Butler, *Proc. Brit. Ceram. Soc.*, **36**, 45-55 (1985).

[3] S. P. S. Badwal and J. Drennan, *J. Mater. Sci.*, **22**, 3231-9 (1987).

[4] M. Aoki, Y-.M. Chiang, I. Kosacki, L. J.-R. Lee, H. Tuller and Y. Liu, *J. Am. Ceram. Soc.*, **79**, 1169-80 (1996).

[5] R. Stevens, Zirconia and Zirconia Ceramics, Magnesium Elektron, Twickenham, 1986.

[6] D. Bingham, P. W. Tasker and A. N. Cormack, *Phil. Mag.* **A 60**, 1-14 (1989).

[7] W. C. Mackrodt, *J. Chem. Soc., Fara. Trans.* 2, **85**, 541-54 (1989).

[8] G. Balducci, J. Kaspar, P. Fornasiero, M. Graziani, M. S. Islam and J. D. Gale, *J. Phys. Chem. B*, **101**, 1750-3 (1997).

[9] G. Balducci, J. Kaspar, P. Fornasiero, M. Graziani and M. S. Islam, *J. Phys. Chem. B*, **102**, 557-61 (1998).

[10] A. Christensen and E. A. Carter, *Phys. Rev. B*, **58**, 8050-64 (1998).

[11] C. A. J. Fisher and H. Matsubara, *Solid State Ion.* **113-115**, 311-8 (1998).

[12] C. A. J. Fisher and H. Matsubara, *Comp. Mater. Sci.* **14**, 177-84 (1999).

[13] C. A. J. Fisher and H. Matsubara, *J. Euro. Ceram. Soc.* **19**, 703-7 (1999).

[14] G. V. Lewis and C. R. A. Catlow, *J. Phys. C: Solid State Phys.* **18**, 1149-1161 (1985).

[15] K. D. Refson, MOLDY 2.14 (MOLecular DYnamics, Version 2.14), University of Oxford, 1999.

[16] H. F. Fischmeister, *Journal de Physique* **C4**, 3-23 (1985).

[17] K. L. Merkle, G.-R. Bai, Z. Li, C.-Y. Song and L. J. Thompson, *Phys. Stat. Sol. A* **166**, 73-89 (1998).

[18] P. W. Tasker, *Phil. Mag. A*, **39**, 119-30 (1979).

[19] D. Sotiropoulou and P. Nikolopoulos, *J. Mater. Sci.*, **26**, 1395-400 (1991).

ACKNOWLEDGMENT

Support from the Special Coordination Funds of the Science and Technology Agency (STA), Japan, is gratefully acknowledged.

(Received December 16, 1999; accepted February 7, 2000)